

## Addendum to "Millimeter spectroscopy in sodium Rydberg states"

C. Fabre, S. Haroche, and P. Goy

*Laboratoire de Physique de l'Ecole, Normale Supérieure, 24 rue Lhomond, 75231 Paris Cedex 05, France*

(Received 10 December 1979)

Using well-stabilized microwave sources in the extended frequency range 50–315 GHz, we have observed very narrow millimeter resonances between Rydberg levels of sodium with principal quantum number  $n$  ranging from 23 to 41. Measurement of the resonance frequencies yields improved values for quantum defects and  $P$ -level fine-structure intervals.

### I. INTRODUCTION

In a previous paper<sup>1</sup>, we have reported the observation of resonances between Rydberg levels of sodium in the millimeter range around 300 GHz. The resolution of these preliminary experiments was limited by the millimeter source characteristics (the oscillator was not stabilized), by the measurement procedure (we used a wave meter), and by intrinsic atomic lifetime and line-broadening effects. Typical linewidths of several MHz, corresponding to a  $10^{-4}$ – $10^{-5}$  resolution were obtained. The quantum-defect values yielded by these experiments had a moderate accuracy of about  $10^{-3}$ . Fine structure could not be determined to better than  $\pm 10$ – $20\%$ . In the conclusion of that study, we pointed out that improvement of the microwave source stability, direct frequency counting, and better shielding of the atoms against perturbations should allow us to greatly improve our resolution. These improvements have been achieved and much narrower resonances obtained, leading to an increase in the precision of spectroscopic data by a factor  $\sim 100$  over our previous results. Very high-resolution two-photon spectroscopic data on  $nS \rightarrow (n+1)S$  transitions have recently been reported elsewhere,<sup>2</sup> along with a discussion of possible application of these experiments to metrology. These measurements have yielded new values of the quantum defects in the  $nS$  series of sodium, with an absolute accuracy of  $4 \times 10^{-7}$ . We report here on measurements of single-photon  $nS \rightarrow n'P$  transitions which have allowed us to determine new values of  $nP$  level quantum defects and fine-structure intervals. The results of the  $nS$  quantum-defect measurements are also briefly summarized for the sake of completeness.

### II. EXPERIMENTAL SETUP

The experiment is performed on an atomic beam of sodium. The atoms are excited to an  $nS$  state by a stepwise process via the  $3P_{1/2}$  level by using two pulsed dye lasers. The laser beams cross

the atomic beam at the entrance of a millimeter semicofocal Fabry-Perot cavity which is coupled to an external millimeter source. The cavity is made of brass and has an aperture of 50 mm in diameter. The distance between the spherical and the plane mirror can be adjusted around the focus ( $\sim 72$  mm). The cavity  $Q$  factor varies from about 25 000 at 55 GHz to 6000 at 120 GHz. After they have crossed the cavity, the excited atoms are detected by selective field ionization according to the technique described in detail in Ref. 1.

The millimeter sources are 7 carcinotrons (Thomson-CSF backwave oscillators) with frequencies  $\nu_c$  centered around 55, 76, 92, 98, 112, 250, and 300 GHz. Each carcinotron is electrically tunable in a wide frequency range: 9, 2, 9, 9, 17, 48, and 37 GHz, respectively. Their output power is typically 50–500 mW. When powered by their stabilized power supply (10 kV  $\pm$  0.1 V Siemel), the carcinotrons have a  $\sim 1$  MHz frequency jitter, which was the main resolution limitation in our earlier work.<sup>1</sup> In order to count the carcinotron frequency and eventually lock it, we use as a reference an  $X$ -band klystron locked on a quartz oscillator. The frequency  $\nu_K$  of the klystron is directly measured with a counter. A homemade mixer using a Schottky diode (Thomson-CSF type DH 382 box BH10; bias 15 mA) generates the  $p$ th harmonic of the klystron ( $6 \leq p \leq 34$ ) and mixes it with the carcinotron radiation. The beat note signal at frequency  $\nu_m = |\nu_c - p\nu_K|$  is amplified and measured either by a counter or by a spectrum analyzer. For high-resolution measurements,<sup>2</sup> this beat note is phase compared to a sweepable local oscillator by a double balanced mixer giving an error signal which is used to phase-lock the carcinotrons. Although the frequency measurements are possible for all our sources, the locking procedure has been achieved so far only up to 120 GHz, due to signal-to-noise problems at higher frequencies. The accuracy of the frequency measurements is a few kHz for locked carcinotrons, a few hundred kHz for free-running carcinotrons.

### III. EXPERIMENTAL RESULTS

#### A. Two-photon $nS \rightarrow (n+1)S$ resonances<sup>2</sup>

These resonances, whose widths were first reported in Ref. 1 to be in the MHz range, become with our improved setup much narrower, with typical linewidth around 10–20 kHz. This resolution is achieved because the Doppler effect (corresponding to a broadening of about 400 kHz) is suppressed by inducing the two-photon transition in the standing wave of the cavity (cancellation of the Doppler shift for two photons propagating in opposite directions). The following transitions have been observed: 32S → 33S, 33S → 34S, 36S → 37S, 39S → 40S, and 40S → 41S. Using the Rydberg formula, the following expression for the  $\epsilon_s(n)$  quantum defects of the  $nS$  level has been obtained ( $32 < n < 41$ ):

$$\epsilon_s(n) = \epsilon_s(\infty) + p_2[n - \epsilon_s(\infty)]^{-2}, \quad (1)$$

with  $\epsilon_s(\infty) = 1.347\,969\,2(4)$  and  $p_2 = 0.061\,37(10)$ .

#### B. Single-photon $nS \rightarrow n'P$ resonances

These resonances are much more sensitive to microwave radiation than the two-photon resonances. The power needed to induce them is so low that cavity tuning is not necessary. The ultimate width of the observed resonances is typically of the order of 500 kHz, to be compared to the ~10 MHz linewidth of the same resonances in our earlier work.<sup>1</sup> The remaining width is due to Doppler effect, residual stray electric-field broadening (~40 mV/cm), and possibly also to partial saturation of the resonance by microwave power. The observed linewidths are in general large enough for the carcinotron to be operated in the unlocked frequency mode. We report here on either  $nS \rightarrow n'P$  or  $nS \rightarrow (n+1)P$  transitions,

all corresponding to absorption of microwave (the  $P$  level lies above the  $S$  one in energy). Some  $nS \rightarrow (n-1)P$  transitions in emission, which are not reported here, have also been observed including six transitions on which maser action has been obtained.<sup>3,4</sup>

Tables I and II give the measured frequencies ( $nS \rightarrow n'P$ ) for  $nS \rightarrow n'P_{1/2}$  and  $nS \rightarrow n'P_{3/2}$  ( $n' = n$  or  $n+1$ ) transitions, respectively. From these values, one can deduce the quantum defects  $\epsilon_p(n')$  according to the Rydberg formula:

$$\nu_c(nS \rightarrow n'P)/R_{Na} = [n - \epsilon_s(n)]^{-2} - [n' - \epsilon_p(n')]^{-2}, \quad (2)$$

where  $\epsilon_s(n)$  is given by Eq. (1) and  $R_{Na}$  is the Rydberg constant for Na expressed in frequency units:

$$\begin{aligned} R_{Na} &= cR_\infty[1 + m_e/(M_{Na} + 10m_e)]^{-1} \\ &= 3.289\,763\,408(20) \times 10^{15} \text{ Hz} \end{aligned}$$

( $R_\infty$ : Rydberg constant;  $c$ : light velocity;  $M_{Na}$  and  $m_e$ : sodium nucleus and electron mass respectively).

The precision of  $\epsilon_p(n')$ ,—about 1 part in  $10^5$ —is limited by the uncertainty of  $\nu_c$ ,  $\delta\nu_c$ . This uncertainty—typically 500 kHz to 1 MHz—reflects the finite width of the resonances and residual uncontrolled Stark and Zeeman effects. Figure 1 shows a least-squares fit of the experimental values  $\epsilon_{p_{1/2}}(n)$  and  $\epsilon_{p_{3/2}}(n)$  versus  $n^{*-2}$ , where  $n^* \simeq n - 0.855$  is the rounded effective quantum number. From these fits, the following formulas are obtained:

$$\epsilon_{p_{1/2}}(n) = \epsilon_{p_{1/2}}(\infty) + q_{1/2}[n - \epsilon_{p_{1/2}}(\infty)]^{-2}, \quad (3)$$

with  $\epsilon_{p_{1/2}}(\infty) = 0.855\,424(6)$  and  $q_{1/2} = 0.1222(2)$ , and

$$\epsilon_{p_{3/2}}(n) = \epsilon_{p_{3/2}}(\infty) + q_{3/2}[n - \epsilon_{p_{3/2}}(\infty)]^{-2}, \quad (4)$$

with  $\epsilon_{p_{3/2}}(\infty) = 0.854\,608(3)$  and  $q_{3/2} = 0.1220(2)$ .

TABLE I. Spectroscopic data for  $nS \rightarrow n'P_{1/2}$  transitions. The first column indicates the quantum number  $n'$  of the  $P$  level of interest. The second column gives the transition observed. The transition frequency  $\nu_{c_{1/2}}$  and its experimental error  $\delta\nu_{c_{1/2}}$  are given in the third and fourth columns, respectively. The quantum defects  $\epsilon_{p_{1/2}}$  deduced from Eqs. (1) and (2) are tabulated in the fifth column. The difference between the observed frequency  $\nu_{c_{1/2}}$  and the value  $\nu'_{c_{1/2}}$  deduced from Eqs. (1), (2) and (3) is given in the sixth column. All frequencies are expressed in MHz.

$n'$	Transition	$\nu_{c_{1/2}}$	$\delta\nu_{c_{1/2}}$	$\epsilon_{p_{1/2}}$	$\nu_{c_{1/2}} - \nu'_{c_{1/2}}$
23	23S → 23P <sub>1/2</sub>	308 621.93	0.5	0.855 672 5(8)	0.37
24	24S → 24P <sub>1/2</sub>	269 926.26	0.5	0.855 652 6(10)	-0.25
25	25S → 25P <sub>1/2</sub>	237 440.70	1.3	0.855 630 4(20)	1.5
32	32S → 32P <sub>1/2</sub>	109 862.90	6.3	0.855 540 1(290)	2.2
33	33S → 33P <sub>1/2</sub>	99 848.75	0.6	0.855 542 9(30)	-0.1
34	34S → 34P <sub>1/2</sub>	91 018.41	1.5	0.855 530 3(80)	0.9
35	34S → 35P <sub>1/2</sub>	263 859.26	0.3	0.855 528 0(20)	0.1
36	35S → 36P <sub>1/2</sub>	241 496.14	1	0.855 521 7(70)	0.2
36	36S → 36P <sub>1/2</sub>	76 248.20	0.5	0.855 525 4(40)	-0.37

TABLE II. Spectroscopic data for  $nS \rightarrow n'P_{3/2}$  transitions. Same presentation as in Table I. The calculated values  $\nu'_{c_{3/2}}$  are obtained from Eq. (4).

$n'$	transition	$\nu_{c_{3/2}}$	$\delta\nu_{c_{3/2}}$	$\epsilon_{P_{3/2}}$	$\nu_{c_{3/2}} - \nu'_{c_{3/2}}$
23	$23S \rightarrow 23P_{3/2}$	309 116.56	0.7	0.854 856 1(10)	0.4
24	$24S \rightarrow 24P_{3/2}$	270 359.46	0.3	0.854 836 3(5)	-0.3
25	$25S \rightarrow 25P_{3/2}$	237 820.77	0.6	0.854 817 3(10)	0
32	$32S \rightarrow 32P_{3/2}$	110 038.73	1.6	0.854 732 8(70)	0.2
33	$33S \rightarrow 33P_{3/2}$	100 010.30	0.4	0.854 727 4(20)	-0.25
34	$34S \rightarrow 34P_{3/2}$	91 165.86	1	0.854 714 2(50)	0.9
35	$34S \rightarrow 35P_{3/2}$	263 993.93	0.3	0.854 713 2(20)	-0.1
36	$35S \rightarrow 36P_{3/2}$	241 619.94	0.3	0.854 704 9(20)	0.3
36	$36S \rightarrow 36P_{3/2}$	76 372.00	0.5	0.854 708 6(20)	0.3

In the last columns of Tables I and II, the measured frequencies  $\nu_c$  have been compared to the values  $\nu'_c$  computed according to Eqs. (1), (2), (3), and (4). The agreement—well within the experimental errors—is quite good. The formulas [Eqs. (3) and (4)] can thus be trusted to give accurate values of the quantum defect of any  $nP$  level of Na for  $n$  in the  $n \geq 13$  range. For lower  $n$  values, higher-order terms in the expansion in even powers of  $n^{*-1}$  are expected to start contributing significantly in the formulas.<sup>5</sup> These

new quantum-defect values are in good agreement—within experimental errors—with the less precise data given in previous works.<sup>1,5,6</sup>

Finally, we give in Table III the experimental fine-structure intervals  $\Delta F(n)$  deduced from the difference between the transition frequencies for corresponding  $P_{3/2}$  and  $P_{1/2}$  sublevels. These values fit the following empirical formula expressed in terms of the rounded effective quantum number  $n^* = n - 0.855$ :

$$\Delta F(n) = An^{*-3},$$

where

$$A = (5.367 \pm 0.005) \times 10^6 \text{ MHz}. \quad (5)$$

Some of the  $P$ -states fine-structure intervals tabulated in this paper had been previously measured either by us in our preliminary work<sup>1</sup> or by Cooke *et al.*<sup>6</sup> on microwave  $nP - n'd$  transitions. Some have also been recently determined by cavity tuning of Rydberg atom masers emitting on  $nS - (n-1)P$  transitions.<sup>3,4</sup> Our present values

TABLE III. Fine-structure intervals  $\Delta F(n)$  of  $nP$  levels. The principal quantum numbers, measured fine-structure intervals  $\Delta F$ , experimental errors  $\delta F$ , and difference between measured ( $\Delta F$ ) and calculated ( $\Delta F'$ ) values are given in columns 1 to 4. All frequencies are in MHz. The calculated values are obtained from Eq. (5).

$n$	$\Delta F(n)$	$\delta F$	$\Delta F - \Delta F'$
23	494.63	1.2	0.43
24	433.20	0.8	0.33
25	380.07	1.9	-1.22
32	175.80	8	-1.86
33	161.50	1	-0.08
34	147.40	2.5	0.01
35	134.67	0.6	-0.15
36	124.20	1	0.57
36	123.80	1.3	0.17

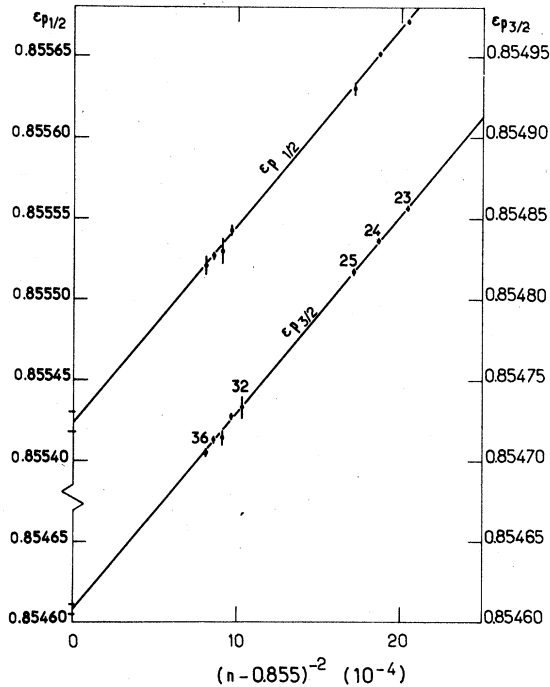


FIG. 1. Variation versus  $1/n^{*2}$  of the quantum defects  $\epsilon_{P_{1/2}}$  (upper; scale on the left) and  $\epsilon_{P_{3/2}}$  (lower; scale on the right).  $n^*$  is the rounded effective quantum number  $n - 0.855$ . Each value of  $\epsilon_p$  is given with its error bar; The solid lines correspond to Eqs. (3) and (4).

are more precise than and in good agreement with all these other determinations (data agree within the experimental errors quoted in these works).

## ACKNOWLEDGMENTS

We are grateful to Dr. R. Adde and Dr. A. Clairon for the loan of equipment.

- 
- <sup>1</sup>C. Fabre, S. Haroche, and P. Goy, *Phys. Rev. A* **18**, 229 (1978).  
<sup>2</sup>P. Goy, C. Fabre, M. Gross, and S. Haroche, *J. Phys. B* **13**, L83 (1980).  
<sup>3</sup>S. Haroche, C. Fabre, P. Goy, M. Gross, and J. M. Raimond, *Laser Spectroscopy IV*, edited by H. Walther

- and K. Rothe (Springer, Berlin, 1979), p. 224.  
<sup>4</sup>M. Gross, P. Goy, C. Fabre, S. Haroche, and J. M. Raimond, *Phys. Rev. Lett.* **43**, 343 (1979).  
<sup>5</sup>P. Risberg, *Ark. Fys.* **41**, 583 (1956).  
<sup>6</sup>W. E. Cooke, T. F. Gallagher, R. M. Hill, and S. A. Edelstein, *Phys. Rev. A* **16**, 2473 (1977).